Journal of Solid State Chemistry 182 (2009) 2801–2805

Contents lists available at ScienceDirect

Journal of Solid State Chemistry

journal homepage: www.elsevier.com/locate/jssc

In-situ oxidation of block copolymer for producing copper oxalate or copper oxide nanowires in mesoporous channels

Jiang Li [1], AiGuo Kong [1], WenJuan Wang, XinHua Zhao, Fan Yang, YongKui Shan *

Department of Chemistry, East China Normal University, ShangHai City 200062, PR China

ARTICLE INFO

Article history:
Received 16 May 2009
Received in revised form
21 July 2009
Accepted 24 July 2009
Available online 3 August 2009

Keywords:
Mesoporous
Nanowire
Copper oxide
Copper oxalate
Hydrogen storage

ABSTRACT

Copper oxalate nanowires inside the channels of mesoporous SBA-15 are created by in-situ oxidation of block copolymer in as-prepared SBA-15 samples. The pyrolysis of CuC_2O_4/SBA-15 composites under different conditions results in the formation of CuO or Cu_2O nanowires encapsulated in the nanoscale channels. The appearance, structure and composition of these materials are characterized by the X-ray power diffraction, transmission electron microscopy, N_2 adsorption–desorption isotherms, infrared spectra and inductive coupled plasma emission spectra. CuC_2O_4, CuO and Cu_2O nanomaterials filled in the channels of SBA-15 have been proven to possess the electrochemical hydrogen storage capacities of 102, 165 and 231 mAh/g in the second cycle, respectively, and are expected to have a high potential for use in practical applications.

1. Introduction

Basing on the "host-guest" chemistry, numerous functional materials can be created by introducing metal oxide or metal complex into mesoporous channels, and which often showed the unique applications in catalysis, optics, electrics, magnetics and nanoscale devices, etc. [1,2]. The integration of 1D nanowires into the well-defined mesoporous channels have attracted growing attentions [3]. Many inorganic nanowire materials such as metal, metal oxide, metal sulfide and organic macromolecular polymer nanowires have been successfully incorporated into the mesoporous silica channels by the special methods [4–9]. However, there are no reports on metal oxalate nanowires inside mesoporous channels [10–12]. The reason is mainly derived from two challenges: (1) the remarkable difficulty in introducing two different precursor species into the mesopores and (2) how to avoid the aggregation of these precursors in the opening channels and effectively increase their infilling amount [13]. Moreover, copper oxide supported on the mesoporous silica has been obtained by the direct-synthesis or post-synthesis methods [14–16], and which exhibited the enhanced catalytic activity in many heterogeneous oxidation reactions [17,18]. However, few studies were mentioned on the synthesis of copper oxide nanowires encapsulated in mesoporous materials. Obviously, it is difficult for the routine impregnation method to obtain copper oxalate and copper oxide nanowires inside mesoporous channels.

The block copolymer surfactant is extensively used as a template in the synthesis of mesoporous materials, which are often removed from the products by calcination or extraction after defining the wall structure of mesoporous materials. Recently, Zhu [19,20] and Yue et al. [21] directly infiltrated guest species into the confined space between the silica wall and the template aggregates in the as-made SBA-15 to obtain novel catalysts or CO_2-capture materials. Li et al. prepared mesoporous carbon by the pyrolysis of silica/triblock copolymer/sucrose composites [22]. It is very attractive to sufficiently explore the utilization of such polymer materials in as-prepared mesoporous silica.

In the present work, block copolymer material in as-made samples of SBA-15 is used as a reactant, which is oxidized to $C_2O_4^{2-}$ in a special aqueous solution containing Cu^{2+}. As a result, copper oxalate nanowires are in-situ produced in the mesoporous silica channels (which is referred to as CuC_2O_4/SBA-15). CuO and Cu_2O nanowires embedded in mesoporous silica (referred to as CuO/SBA-15 and Cu_2O/SBA-15) are also obtained by heating CuC_2O_4/SBA-15. These copper-containing materials reveal good textural properties and ordered mesostructures, and possess 102, 165 and 231 mAh/g electrochemical hydrogen storage capacity in the second cycle, respectively.

2. Experimental

2.1. Synthesis

In a typical preparation of materials, as-prepared samples of mesoporous SBA-15 without hydrothermal treatment were

* Corresponding author. Fax: +86 21 62233503.
E-mail address: ykshan@chem.ecnu.edu.cn (Y. Shan).
[1] Joint first author. Both authors contributed equally to this work.

0022-4596/$ - see front matter © 2009 Elsevier Inc. All rights reserved.
doi:10.1016/j.jssc.2009.07.050

obtained following the literatures [23]. Dried samples of hybrid mesoporous materials of 4.0 g, 8.0 g $CuSO_4 \cdot 5H_2O$ and 8.0 g water were mixed, stirred for 2 h, and then the mixtures were dried at 353 K. After that, the resultant solid mixtures were added into the solution containing 7.5 g $Al(NO_3)_3 \cdot 5H_2O$, 6.2 g H_3PO_4 (85 wt%) and 30.0 g water, and subsequently heated at 373 K for two days in a sealed autoclave. Finally, mesoporous CuC_2O_4/SBA-15 products were collected and treated by filtering, washing with water six times, and drying at 373 K. The mesoporous CuO /SBA-15 materials were obtained through the calcination of CuC_2O_4/SBA-15 samples at 623 K for 4 h in air at a heating rate of 1 K/min. For the preparation of mesoporous Cu_2O/SBA-15, CuO/SBA-15 samples in a crucible were covered up in active carbon particles, and then heated at 973 K for 8 h in air.

2.2. Characterization

The X-ray diffraction data of all samples were collected in θ–2θ mode using a Rigaku Corporation D/MAX 2200PC diffractometer equipped with Cu$K\alpha$ ($K = 0.1541$ nm) radiation, operating at 32 kV, 20 mA for 2θ low-angle (0.5–5°) and 40 kV, 40 mA for 2θ high-angle (10–70°). The porous textures of mesoporous materials were analyzed from nitrogen adsorption–desorption isotherms at 77 K by using a Micromeritics ASAP 2000 system. Transmission electron microscopy (TEM) images were taken with a JEOL JEM-200CX transmission electron microscope using an accelerating voltage of 200 kV. The amounts of Cu, Si, Al and P in the synthesized samples were determined by ICP-AES analysis on a thermo elemental PERKIN-ELMER PLASMA-2000 spectrometer. Infrared spectra (FT-IR) were recorded on a Nexus-870 Fourier-transform spectrophotometer from KBr pellets with a measuring range 400–4000 cm^{-1}.

The electrochemical measurements of these samples were performed in a three-electrode cell using 6 mol/l KOH as electrolyte. The mesoporous SBA-15 samples containing copper species, $Ni(OH)_2$/NiOOH and Hg/HgO (1 M NaOH, +0.114 V) were used as the working electrode, the counter electrode and the reference electrode, respectively. The working electrode was prepared as follows: 0.02 g of the mesoporous SBA-15 samples containing copper species, 0.01 g of acetylene black powders and 0.11 g of poly-tetrafuroethylene solution (30 wt%) were mixed. These homogeneous mixtures were smeared onto the foam nickel sheet and pressed at 11 MP for 2 min. The counter electrode $Ni(OH)_2$/NiOOH was prepared by the similar procedures using 0.1 g NiOOH, 0.05 g acetylene black powders and 0.055 g poly-tetrafuroethylene solution (30 wt%). The working electrodes were charged for 6 h at a current density of 100 mA/g, and were discharged to −0.2 V (vs Hg/HgO, +0.114 V) at a current density of 60 mA/g. The electrochemical hydrogen storage capacities were calculated according to the mass of copper species in the samples.

3. Results and discussion

3.1. Mesostructures of these Cu-containing materials

A very sharp (100) diffraction peak together with well-resolved higher order (110) and (200) reflections in the low-angle XRD pattern of CuC_2O_4/SBA-15 materials (Fig. 1A-a) indicate that it has a long-range ordered 2D hexagonal (*P6mm*) structure. CuO/SBA-15 materials also show the well hexagonal mesostructure regularity (Fig. 1A-b). Comparatively, the diffraction peaks of mesoporous Cu_2O/SBA-15 (Fig. 1A-c) decreased in the intensity and had a little shift to high diffraction angles.

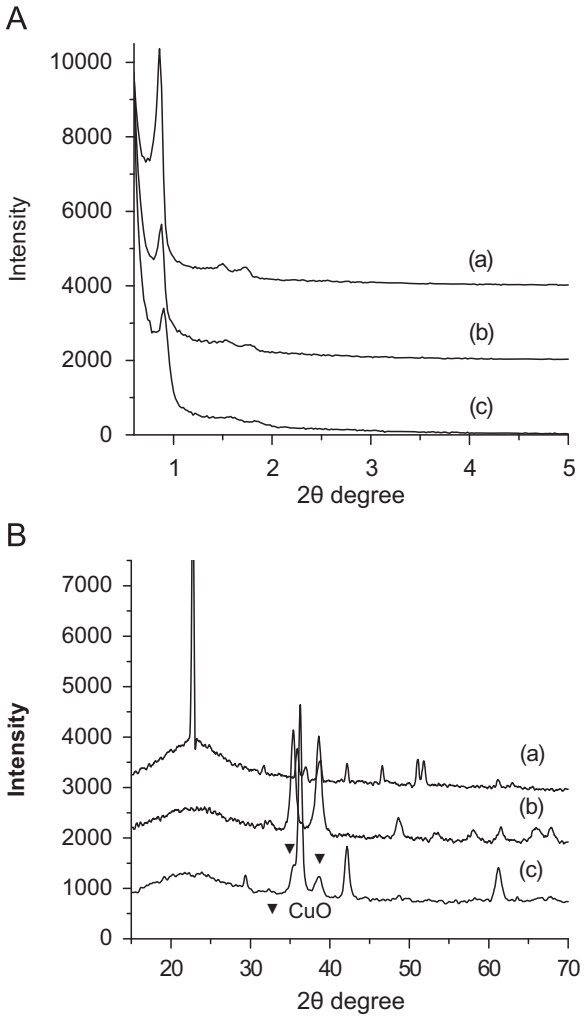

Fig. 1. The low-angle (A) and high-angle (B) XRD patterns of CuC_2O_4/SBA-15 (a), CuO/SBA-15 (b) and Cu_2O/SBA-15 (c).

The corresponding high-angle XRD patterns of these samples shown in Fig. 1B testify that crystalline CuC_2O_4 have the orthorhombic phase (JCPDS 46-0856), in agreement with the previous results reported by us [24]. The high-angle XRD patterns also reveal that CuC_2O_4 materials were converted to crystalline CuO with monoclinic phase (JCPDS 45-0937). The pyrolysis of CuO/SBA-15 under reductive atmosphere results in the formation of cubic phase Cu_2O materials (JCPDS 05-0667) within SBA-15 with a small amount of CuO(▼).

TEM images of CuC_2O_4/SBA-15, CuO/SBA-15 and Cu_2O/SBA-15 materials fully exhibit their order hexagonal mesostructures (Fig. 2). TEM images (Fig. 2a and b) of CuC_2O_4/SBA-15 suggest that a large amount of CuC_2O_4 has been introduced into the pores of SBA-15. In comparison with the pore walls, the equal or darker contrast grade in the pore channels shows the more continuous black solid lines within the mesoporous channels. Such black lines are believed to be CuC_2O_4 nanowires because their growth direction is analogous to the pore configuration [25,26]. A similar phenomenon is also founded in the samples of mesoporous CuO/SBA-15 materials (Fig. 2c and d). The intense contrast can more accurately recreate the original image of CuO nanowires in the corresponding TEM images, resembling the TEM images of SnO_2 nanowires in the nanoscale-channels [25]. The corresponding electron diffraction reveals the polycrystalline property of CuO materials within SBA-15 (Fig. 2c inset). TEM images in Fig. 2e and f illustrate that Cu_2O nanowires are obtained in the channels of

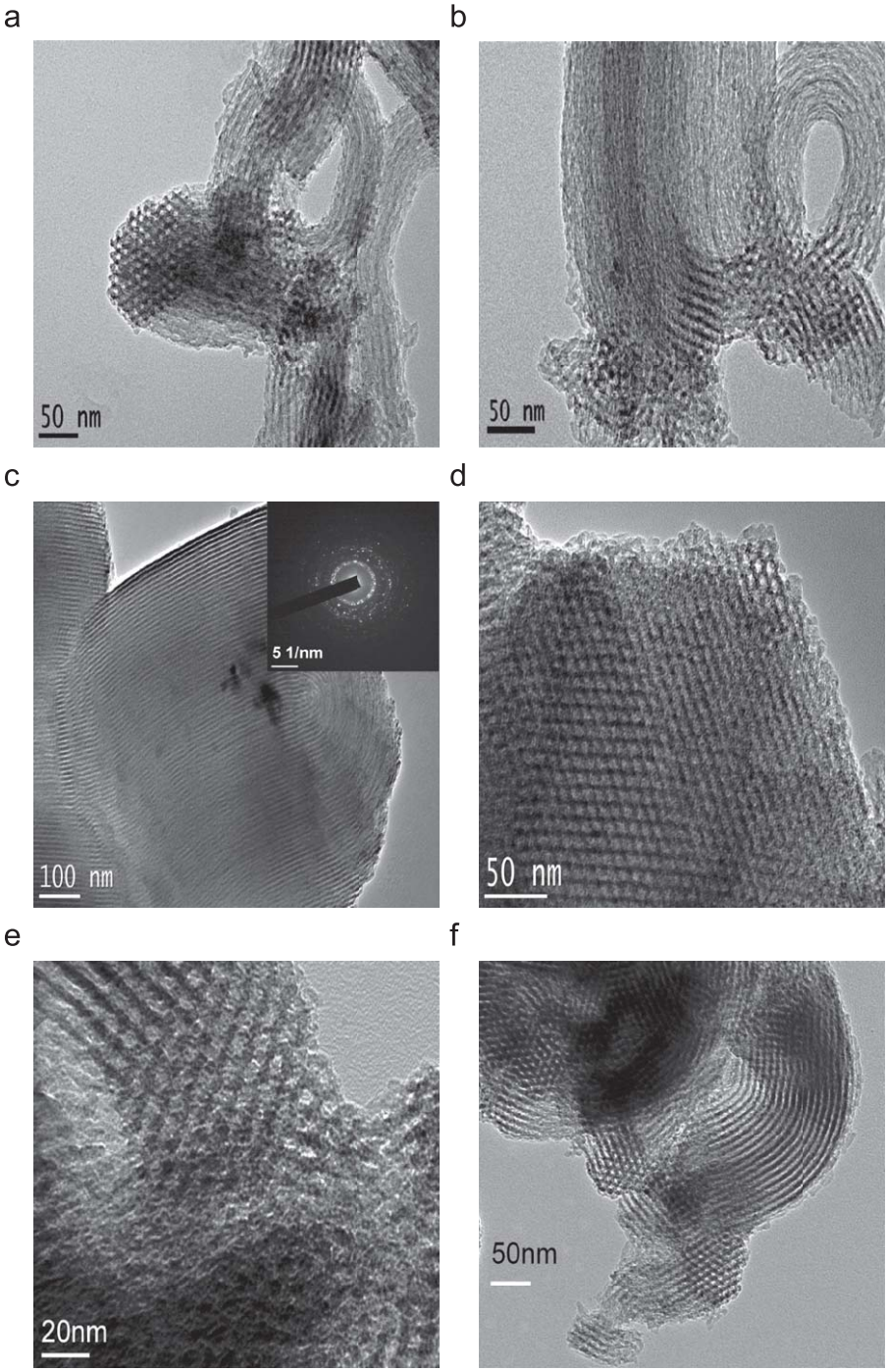

Fig. 2. TEM images of the copper species encapsulated in mesoporous SBA-15 materials recorded along the different directions: (a, b) copper oxalate(CuC_2O_4), (c, d) copper oxide(CuO) and (e, f) cupper oxide(Cu_2O). Inset is the corresponding electron diffraction of CuO/SBA-15 materials.

SBA-15. It is notable that few CuC_2O_4, CuO and Cu_2O bulk particles are observed on the external surface of mesoporous silica and very different from the general impregnation techniques, in which the uncontrolled stack of bulk copper species on the external surface of mesoporous silica is usually serious [27,28].

The corresponding FT-IR spectra (Fig. 3) show that the bands between 2800 and 3000 cm^{-1} assigning to C–H stretching vibration of block copolymer in as-made SBA-15 particles remarkably decrease in mesoporous CuC_2O_4/silica samples. When further compared with two spectra (a and b in Fig. 3), the increased intensity of around 1640, 823 cm^{-1} (characteristic bands of $C_2O_4^{2-}$) and the decreased intensity of around 1400 cm^{-1} mainly assigning to C–H bending vibration (Fig. 3, a) are obviously observed. New bands at 1364 and 1320 cm^{-1} (characteristic bands of $C_2O_4^{2-}$) are also found in the FT-IR spectra of CuC_2O_4/SBA-15. According to the characters of the FT-IR spectra and the corresponding XRD patterns, it is concluded that most of block copolymer were in-situ oxidized to CuC_2O_4. The ICP-AES analysis indicates that Cu content in CuC_2O_4/SBA-15, CuO/SBA-15 and Cu_2O/ SBA-15 are about 11.1, 15.2 and 15.8 wt%.

Interestingly, no aluminum or phosphorus species are remained in the final products, in agreement with the IR and XRD results [24].

These experimental results demonstrate that $Cu_2C_2O_4$, CuO and Cu_2O nanowire materials in mesoporous SBA-15 channels have been successfully prepared. As we know, metal oxalate nanomaterials incorporated in the mesoporous materials are not reported.

3.2. Textural properties of these materials

Isothermal N_2 absorption–desorption analyses (Fig. 4) are employed to investigate the textural property of these materials, and the experimental data are listed in Table 1. The results reveal that CuC_2O_4/SBA-15, CuO/SBA-15 and Cu_2O/SBA-15 exhibit the typical type-IV absorption–desorption isotherms, which is similar to that of pure mesoporous SBA-15. Mesoporous CuC_2O_4/SBA-15 materials possess 324 m^2/g surface area, 0.52 cc/g pore volume and narrow pore size distribution centered at 6.2 nm. Comparatively, mesoporous CuO/SBA-15 shows a higher surface area (365 m^2/g) and a larger pore volume (0.63 cc/g). The increased pore volume and surface area of CuO/SBA-15 are mainly due to the decomposition of CuC_2O_4 at 623 K and leaving behind some spaces. In comparison with the mesoporous CuC_2O_4/SBA-15 and CuO/SBA-15, Cu_2O/SBA-15 materials have the smaller pore volume and the lower surface area, which may be attributed to the severely shrinking of silica framework and the mesostructure damage when heating at high temperature. Its pore size distribution is also more extensive and centered at 5.3 or 6.2 nm. In addition, in contrast to 1.17 cm^3/g pore volume and 807 m^2/g surface area of pure SBA-15 silica, the pore volume and surface area of CuC_2O_4/SBA-15, CuO/SBA-15 and Cu_2O/SBA-15 materials remarkably decreased. It suggests the effective filling of these copper species in the channels.

All the results have indicated that copper species were embedded in mesoporous channels in the form of nanowires. The reason for the formation of these nanowire materials may be that a large amount of CuC_2O_4 was in-situ produced in the channel. After the hybrid mesoporous silica is obtained, the excrescent block copolymer templates can be easily removed by simple washing, and thus the residual block copolymer is almost embedded in the mesoporous channels. These block copolymer materials can be slowly oxidized to $C_2O_4^{2-}$ in a hot solution containing Cu^{2+}, Al^{3+}, PO_4^{3-}, SO_4^{2-} and NO^{3-} and in sequence, $C_2O_4^{2-}$ rapidly reacted with Cu^{2+} in the mesoporous channels. As a result, the controllable production and deposition of CuC_2O_4 for the formation of nanowire in the mesoporous channels was achieved, and then CuC_2O_4 nanowires can be transformed into the CuO and Cu_2O nanowires under the specified conditions.

To explore the effect of PO_4^{3-}, Al^{3+} on the formation of CuC_2O_4, the oxidation of block polymer in as-made SBA-15 was investigated in some systems containing different components such as $CuSO_4$, $CuSO_4$–HNO_3, $CuSO_4$–HCl and $CuSO_4$–HCl–H_2O_2. The results show that few samples of CuC_2O_4 can be produced in these systems not containing $Al(NO_3)_3$ and H_3PO_4. These facts illuminate that block polymer template may be mainly oxidized by NO^{3-} and PO_4^{3-}, Al^{3+} in this acid solution containing Cu^{2+} probably formed a chemical stable system with special catalytic

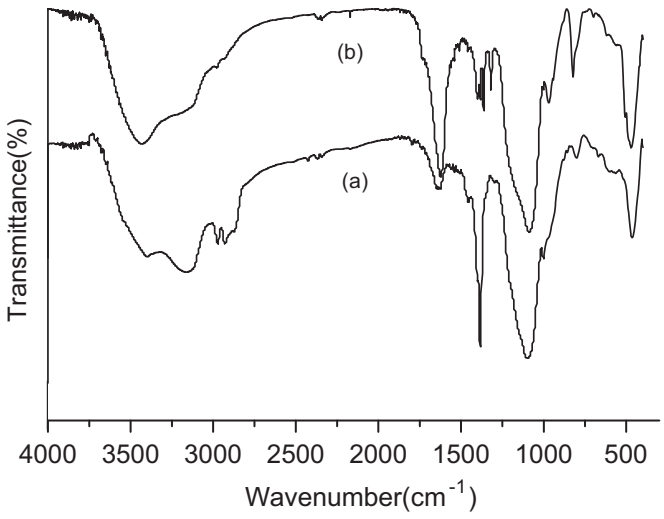

Fig. 3. FT-IR spectra of copper species embedded in mesoporous SBA-15 materials: (a) as-prepared SBA-15 and (b) CuC_2O_4/SBA-15.

Table 1
The textural properties of copper-containing nanowires within mesoporous SBA-15.

Materials	d_{100} (nm)	Cu content (wt%)	BET (m^2/g)	V_{tot} (cm^3/g)	D (nm)
SBA-15	10.4		807	1.17	8.0
CuC_2O_4/SBA-15	10.3	11.1	324	0.52	6.2
CuO/SBA-15	10.0	15.2	365	0.63	6.2
Cu_2O/SBA-15	9.8	15.8	312	0.49	5.3 6.2

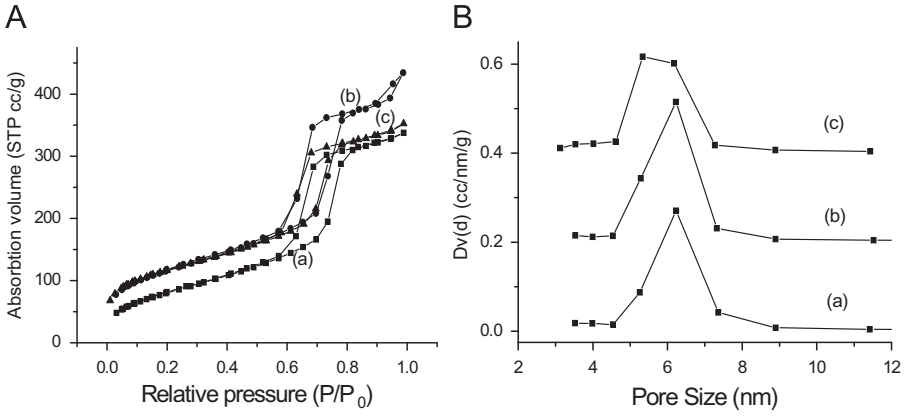

Fig. 4. The N_2 adsorption–desorption isotherms (A) and the corresponding pore size distribution curves (B) of mesoporous CuC_2O_4/SBA-15 (a), CuO/SBA-15 (b) and Cu_2O/SBA-15 (c).

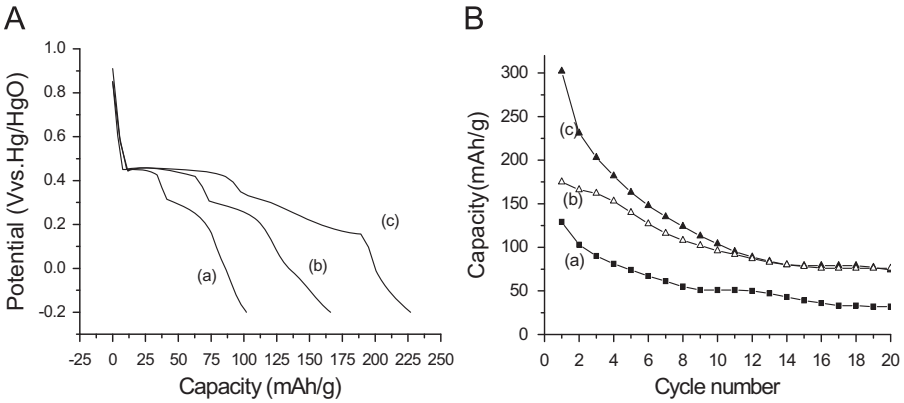

Fig. 5. The second discharge (A) curves and cycle life (B) curves of mesoporous CuC_2O_4/SBA-15 (a), CuO/ SBA-15 (b) and Cu_2O/SBA-15 (c).

redox properties. More efforts will be needed to clarify the special roles of $Al(NO_3)_3$ and H_3PO_4 and reaction mechanism.

3.3. The electrochemical hydrogen storage performance

Copper oxide nanomaterials have attracted more attention, owing to their potential applications in catalysis, gas sensors, lithium ion electrode materials and photo electrochemical materials. Recently, $Cu(OH)_2$ and CuO nanoribbon arrays with high surface have demonstrated their excellent hydrogen storage performance [29,30]. The electrochemical hydrogen storage ability of these prepared copper-containing nanowire materials is also investigated. Their second discharge curves are shown in Fig. 5A. CuC_2O_4/SBA-15 possesses a 102 mAh/g electrochemical hydrogen storage capacity in the second cycle. For CuO/SBA-15, it shows a 165 mAh/g capacity, similar to the results of CuO nanoribbon arrays reported by Gao et al. [30]. Comparatively, Cu_2O/ SBA-15 materials exhibit the higher hydrogen storage capacity in the second cycle, and have a 231 mAh/g capacity in our electrochemical measurement experiments. The cycle life of these materials is shown in Fig. 5B. After being cycled 20 times, the discharging capacity of CuC_2O_4/SBA-15 materials remains more than 30 mAh/g. Both copper oxide nanowire materials testify the proximal discharging capacity around 70 mAh/g. These results indicate that these copper-based nanomaterials may be potentially applied in the electrochemical hydrogen storage. However, currently little is known about the electrochemical hydrogen storage process in copper-based nanomaterials electrode except that the hydrogen storage performance of materials was related to their composition and microstructure. It is still an interesting subject to find out which step is the rate-controlling step in the electrochemical charge–discharge process of copper-based nanomaterials, and the detailed electrochemical hydrogen storage mechanism is worth deep investigation.

4. Conclusions

In conclusion, CuC_2O_4 nanowires encapsulated in the mesoporous channels were created by a special method, in which the controllable deposition of CuC_2O_4 in pore channels was achieved through the in-situ oxidation of block polymer in a special solution. CuO and Cu_2O nanowires in the channel of SBA-15 were also obtained by the pyrolysis of CuC_2O_4/SBA-15. These materials showed the good electrochemical hydrogen storage performance and were expected to have a high potential for use in practical applications

Acknowledgment

We thank key project of Shanghai Science and Technology Committee (no. 05JC14070, 06DZ05025, 08JC1408600) for financial support.

References

[1] N. Petkov, T. Bein, F. Laeri, F. Schueth, U. Simon, M. Wark (Eds.), Host-Guest-Systems Based on Nanoporous Crystals, Wiley, Weinheim, Germany, 2003, pp. 393–409.
[2] Y. Wan, H. Yang, D. Zhao, Acc. Chem. Res. 39 (2006) 423–432.
[3] Y.N. Xia, P.D. Yang, Y.G. Sun, Y.Y. Wu, B. Mayers, B. Gates, Y.D. Yin, F. Kim, Y.Q. Yan, Adv. Mater. 15 (2003) 353–389.
[4] T.A. Crowley, K.J. Ziegler, D.M. Lyons, D. Erts, H. Olin, M.A. Morris, J.D. Holmes, Chem. Mater. 15 (2003) 3518–3522.
[5] B. Tian, X. Liu, H. Yang, S. Xie, C. Yu, B. Tu, D. Zhao, Adv. Mater. 15 (2003) 1370–1374.
[6] F. Jiao, A. Harrison, J.C. Jumas, A.V. Chadwick, W. Kockelmann, P.G. Bruce, J. Am. Chem. Soc. 128 (2006) 5468–5474.
[7] K. Jiao, B. Zhang, B. Yue, Y. Ren, S. Liu, S. Yan, C. Dickinson, W. Zhou, H. He, Chem. Commun. 45 (2005) 5618–5619.
[8] K.J. Ziegler, P.A. Harrington, K.M. Ryan, T. Crowley, J.D. Holmes, M.A. Morris, J. Phys. Condens. Matter 15 (2003) 8303–8314.
[9] F. Gao, Q. Lu, X. Liu, Y. Yan, D. Zhao, Nano Lett. 1 (2001) 743–748.
[10] K. Melis, V. DeVos, P. Jacobs, F. Verpoort, J. Mol. Catal. A 169 (2001) 47–49.
[11] X.G. Zhou, X.Q. Yu, J.S. Huang, S.G. Li, L.S. Li, C.M. Che, Chem. Commun. 18 (1999) 1789–1790.
[12] D. Das, C.M. Tsai, S. Cheng, Chem. Commun. 5 (1999) 473–474.
[13] F. Gao, Q. Lu, D. Zhao, Adv. Mater. 15 (2003) 739–742.
[14] Z. Wu, Y. Wang, W. Huang, J. Yang, H. Wang, J. Xu, Y. Wei, J. Zhu, Chem. Mater. 19 (2007) 1613–1625.
[15] K.M. Parida, D. Rath, Appl. Catal. A Gen. 321 (2007) 101–108.
[16] L. Wang, A. Kong, B. Chen, H. Ding, Y. Shan, M. He, J. Mol. Catal. A Chem. 230 (2005) 143–150.
[17] B. Chou, J.L. Tsai, S. Cheng, Microporous Mesoporous Mater. 48 (2001) 309–317.
[18] K. Bachari, O. Cherifi, Catal. Commun. 7 (2006) 926–930.
[19] Y.L. Wei, Y.M. Wang, J.H. Zhu, Z.Y. Wu, Adv. Mater. 15 (2003) 1943–1945.
[20] Y. Wang, Z. Wu, L. Shi, J. Zhu, Adv. Mater. 17 (2005) 323–327.
[21] M. Yue, Y. Chun, Y. Cao, X. Dong, J. Zhu, Adv. Funct. Mater. 16 (2006) 1717–1722.
[22] L.X. Li, H.H. Song, X.H. Chen, Microporous Mesoporous Mater. 94 (2006) 9–14.
[23] D. Zhao, J. Feng, Q. Huo, N. Melosh, G.H. Fredirckson, B.F. Chemlka, G.D. Stucky, Science 279 (1998) 548–552.
[24] A. Kong, H. Wang, X. Yang, Y. Hou, Y. Shan, Microporous Mesoporous Mater. 118 (2009) 348–355.
[25] H. Kim, J. Cho, J. Mater. Chem. 18 (2008) 771–775.
[26] M.H. Huang, A. Choudrey, P. Yang, Chem. Commun. 12 (2000) 1063–1064.
[27] H. Fujiyama, I. Kohara, K. Iwai, S. Nishiyama, S. Tsuruya, M. Masai, J. Catal. 188 (1999) 417–425.
[28] C.C. Pantazis, P.N. Trikalitis, P.J. Pomonis, J. Phys. Chem. B 109 (2005) 12574–12581.
[29] P. Gao, M. Zhang, Z. Niu, Q. Xiao, Chem. Commun. 48 (2007) 5197–5199.
[30] P. Gao, Y. Chen, H. Lv, X. Li, Y. Wang, Q. Zhang, Int. J. Hydrogen Energy 34 (2009) 3065–3069.